Coarse-grained model of tropoelastin self-assembly into nascent fibrils

A. Tarakanova [a,b], J. Ozsvar [c,d], A.S. Weiss [c,d,e,f], M.J. Buehler [a,*]

[a] Laboratory for Atomistic and Molecular Mechanics, Department of Civil and Environmental Engineering, Massachusetts Institute of Technology, Cambridge, MA, USA
[b] Department of Mechanical Engineering and Department of Biomedical Engineering, University of Connecticut, Storrs, CT, USA
[c] School of Life and Environmental Sciences, The University of Sydney, Sydney, NSW, Australia
[d] Charles Perkins Centre, The University of Sydney, Sydney, NSW, Australia
[e] Bosch Institute, The University of Sydney, Sydney, NSW, Australia
[f] Sydney Nano Institute, The University of Sydney, Sydney, NSW, Australia

A B S T R A C T

Elastin is the dominant building block of elastic fibers that impart structural integrity and elasticity to a range of important tissues, including the lungs, blood vessels, and skin. The elastic fiber assembly process begins with a coacervation stage where tropoelastin monomers reversibly self-assemble into coacervate aggregates that consist of multiple molecules. In this paper, an atomistically based coarse-grained model of tropoelastin assembly is developed. Using the previously determined atomistic structure of tropoelastin, the precursor molecule to elastic fibers, as the basis for coarse-graining, the atomistic model is mapped to a MARTINI-based coarse-grained framework to account for chemical details of protein–protein interactions, coupled to an elastic network model to stabilize the structure. We find that self-assembly of monomers generates up to ~70 nm of dense aggregates that are distinct at different temperatures, displaying high temperature sensitivity. Resulting assembled structures exhibit a combination of fibrillar and globular substructures within the bulk aggregates. The results suggest that the coalescence of tropoelastin assemblies into higher order structures may be reinforced in the initial stages of coacervation by directed assembly, supporting the experimentally observed presence of heterogeneous cross-linking. Self-assembly of tropoelastin is driven by interactions of specific hydrophobic domains and the reordering of water molecules in the system. Domain pair orientation analysis throughout the self-assembly process at different temperatures suggests coacervation is a driving force to orient domains for heterogeneous downstream cross-linking. The model provides a framework to characterize macromolecular self-assembly for elastin, and the formulation could easily be adapted to similar assembly systems.

1. Introduction

Elastic fibers are found in the extracellular matrix of vertebrate connective and vascular tissue such as the skin, blood vessels, lungs, elastic ligaments and the heart and bestow tissue with elasticity and resilience [1]. Elastogenesis, the elastic fiber assembly process, begins when tropoelastin monomer molecules, soluble precursors to the mature elastin, are secreted from the cell and self-assemble into bundles [2]. Human tropoelastin is expressed by elastogenic cells and secreted and then processed as a 60-kDa unglycosylated protein [3]. The self-association that tropoelastin undergoes under physiological conditions is referred to as coacervation [4]. As the first stage in the elastic fiber assembly process, coacervation of tropoelastin is key to the proper assembly of elastic fibers and consequent normal tissue

function, while disruption of this process results in disease [5]. In fact, inhibition of coacervation leads directly to decreased elastin formation [6].

As tropoelastin is secreted from the cell, it forms growing spherical globules [7,8]. Below the transition temperature for a given concentration, tropoelastin molecules exist as monomers [4]. As temperature is increased, tropoelastin monomers assemble rapidly, without apparent evidence of intermediate stages as observed in experiment [7,9]. Assembly typically occurs through a very narrow temperature range of less than 5 °C, as evidenced by a sharp spike in turbidity, corresponding to elastin's well-characterized inverse temperature transition [10,11]. As temperature rises, monomers aggregate into microcoacervates, resulting in a rise of solution turbidity [12–14]. Coacervate spherules grow to a size of 2–6 μm, a process that occurs almost immediately [4].

* Corresponding author.
   E-mail address: mbuehler@mit.edu (M.J. Buehler).

Experimentally, assembly at smaller scales is challenging to capture, yet our present work suggests that assembly occurs rapidly yet with the formation of smaller length-scale intermediate clusters of tropoelastin monomers. Initial phase separation and coalescence of monomers is reversible, where dissipation of monomers occurs upon cooling [7]. Coacervates stabilize and mature over time, exhibiting no reversibility into a monomer phase after extended time. Coacervates interact forming isolated filaments, and progressively, bundles. Over hours, elastin fibrils are able to form [12,15–17]. The hierarchical structure of elastic fibers is shown in Fig. 1.

Various earlier studies have considered coacervation in vitro, by attempting to reproduce conditions present in the extracellular matrix upon development or remodeling. Early studies considered hydrolyzed elastin peptides, identifying temperature-dependent aggregation and fiber formation similar to native elastin [12,13,18–20]. Subsequent studies considered synthetic elastin-like polypeptides, based on repeating unit sequences from hydrophobic domains of tropoelastin also showing extensive aggregation and fibril formation, suggesting a key role played by hydrophobic domains in the assembly and polymerization of tropoelastin [21–29]. Aggregation studies of individual hydrophobic tropoelastin domains have been reported subsequently and showed dissimilar behavior [30]. For example, a sequence of domain 18 of tropoelastin coacervated at physiological temperature [31], while domains 20, 24, and 26 aggregated only at high concentration and temperature, suggesting domain-specific roles for aggregation [32–34]. Studies using sequences that capture the alternating nature of hydrophobic and hydrophilic domains in elastin [32,35,36], as well as those using full-length recombinant tropoelastin [37,38] both revealed aggregation and formation of fibrillar structures. Coacervation has been proposed to be the process by which tropoelastin alignment occurs for downstream cross-linking to take place [12,35,39]. Cross-link formation as elastin matures involves specific lysine residues, which can be orientated during the coacervation process for correct alignment of lysine side chains within cross-linking domains.

Few computational models have been proposed to consider elastin self-aggregation, as most have focused on single-molecule structure and dynamics [40–46]. Several studies have considered multichain elastin-like systems; however, they have been limited in number, ranging from two to six chains [47–49], or have considered a system consisting of repetitive domains representative of tropoelastin's hydrophobic domains, neglecting cross-linking domains [50]. In the present study, the full-length monomer of tropoelastin [51] is used as a template for elastin self-aggregation. A model of the coacervation process is constructed to examine the molecular behavior and mechanisms driving the self-association of elastin at time scales that are almost instantaneous (microsecond scales) and therefore inaccessible to experimental measurement. Our model extends the description of coacervation identifying cluster intermediates that form at the nanometer scales, not previously observed in experiment. We find that tropoelastin self-assembly occurs as a two-step process of nucleation and growth events, where linear assembly begins with the formation of a coacervate nucleus, as molecules are driven to interact with one another via specific hydrophobic domains, followed by the growth of the coacervate in a cooperative fashion. The location and movement of specific domains within the molecule as well as the role of water is quantified to identify dominant assembly-driving mechanisms and to evaluate whether molecular orientation takes place in a cooperative fashion for downstream cross-linking.

2. Materials and methods

The template molecular structure of tropoelastin was taken from earlier work [51] as a basis to build a self-assembling system. The atomistic tropoelastin structure is originally computed from the primary protein structure of mature, wild-type human tropoelastin corresponding to residues 27–724 of GenBank entry AAC98394. The sequence is a 60-kDa protein of 698 residues. The equilibrated representative structure from Replica Exchange Molecular Dynamics simulation was chosen as the starting structure.

A combined structure-based and physics-based coarse-graining approach is used, combining the MARTINI force field and an elastic network model into a single representation [52–54]. Such coarse-graining results in simulation times reduced by 2–3 orders of magnitude compared to fully atomistic simulations. Global molecular shape is maintained by the elastic network scaffold, while the MARTINI force field captures the intermolecular and intramolecular interactions of the system. To construct the coarse-grained (CG) models, the atomistic structure was converted into a CG structure using the martinize script [52]. In the MARTINI framework, four heavy atoms are mapped to one interaction center [52,53,55]. For ring-like structures, higher resolution mapping of two-to-one is used. The MARTINI model was coupled with an elastic network through the *ElNeDyn* implementation [54]. The global elastic network stabilizes the structures, while allowing for oscillation about the equilibrium. A global elastic network is created between the backbone beads to conserve the conformation of the structure, where locations of Cα-atoms are used as backbone beads, rather than the center of mass of the peptide plane as used in standard MARTINI. Two backbone beads are connected when they are at least two steps apart along the backbone and when their distance is below the upper cutoff. The elastic bond strength is set at 500 kJ/mol*nm^2 with the upper cutoff at 0.9 nm.

The starting configuration of the self-assembling system was generated by placing forty copies of the CG tropoelastin molecule, randomly distributed, into a CG water box of $50 \times 50 \times 50$ nm^3. The box size exceeded the protein surface by at least 5 nm in each direction. Chloride counterions were added to neutralize the system. Subsequently, 5000 steps of energy minimization using the steepest descent algorithm were performed. Following energy minimization, system relaxation was performed by simulating the system with protein bead position restrained for 25,000 steps, sequentially, using a time step of 5, 10, 15, and 20 fs (corresponding to simulations times of 125, 250, 375, and 500 ps, respectively). Subsequently, position restraints were removed, and the
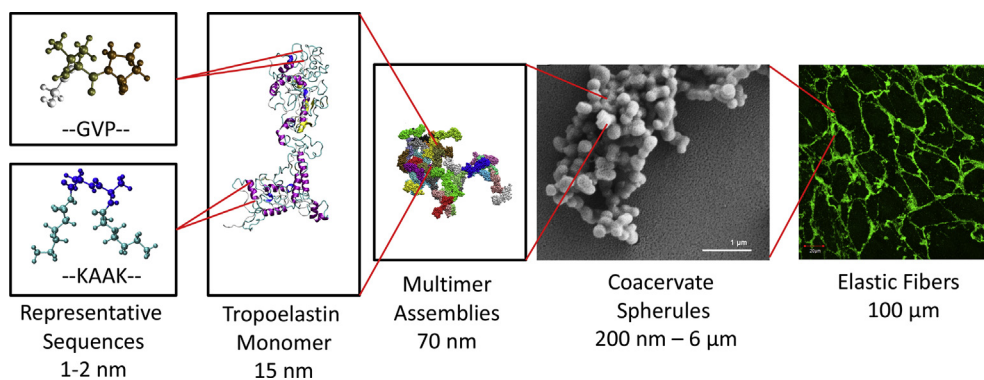
Fig. 1. Overview of the hierarchical structure of elastic fibers. Tropoelastin is composed of alternating GVP-rich hydrophobic domains and hydrophilic K-containing cross-linking domains. The tropoelastin monomer represents the essential building block for elastic fibers. Tropoelastin interacts to form nanoassemblies discussed in this work. Nanoassemblies form into spherical aggregate structures (figure reprinted from Ref. [65] with permission from Elsevier). Spherules assemble onto a microfibrillar scaffold to form an elastic fiber. Figure modified from Ref. [60] with permission from Elsevier.

--GVP--

--KAAK--

Representative Sequences
1-2 nm

Tropoelastin Monomer
15 nm

Multimer Assemblies
70 nm

Coacervate Spherules
200 nm – 6 μm

Elastic Fibers
100 μm

system was simulated for 10 μs, using an integration time step of 20 fs. Because of the smoothing of the energy landscape in any CG simulation scheme, an effective speed-up of dynamics is expected. The expected speed-up of diffusion dynamics of MARTINI water compared to real water is a factor of 4. Because no extensive calibration has been performed for protein systems, however, all reported times are not rescaled by a factor of 4 in this work.

A total of four simulations were performed with different randomized starting positions and velocities at each temperature. All simulations were performed in an NPT ensemble. The system was simulated at three temperatures: 20, 27, and 37 °C. Temperature was maintained using the v-rescale algorithm, with τ_T of 1.0 ps. The Parrinello–Rahman barostat was used to maintain a pressure of 1 bar, with a coupling constant τ_P of 12.0 ps. Periodic boundary conditions were applied. All simulations were performed using the Gromacs version 5.4.1 [56,57] and the MARTINI force field version 2.2 [55]. The *ElNeDyn* model was used to embed the elastic network [54]. All analysis was performed using Gromacs routines and in-house scripts. Visualization of molecular models was performed using Visual Molecular Dynamics 1.9.1 [58] and in-house scripts.

3. Results and discussion

A CG model is constructed, combining the MARTINI framework with an elastic network model, based on the fully atomistic structure of the tropoelastin monomer [51] (Fig. 2a). An elastic network model has been previously shown to capture global domain motions of monomeric tropoelastin [59,60]. Self-assembly is modeled from a randomly distributed system of forty tropoelastin monomers in a periodic water box (Fig. 2b). Four independent runs are performed at each of the three temperatures 20, 27, and 37 °C, from uniquely random starting configurations of the monomers (Fig. 2c). Monomers are simulated over 10 μs, undergoing a multistep assembly process. We find that monomers assemble into aggregates, first forming clusters (Fig. 3a–c) at 20, 27, and 37 °C, respectively. At all temperatures, cluster formation is rapid, with a plateau in cluster size observed between 4 and 6 μs. Still, at 37 °C compared to 20 °C, cluster formation occurs more quickly, and clustering is smoothed at long time scales at higher temperature. Aggregates represent low energy states for tropoelastin monomers. Higher temperature accelerates the aggregation process and stabilizes cluster formation, demonstrated by smoother clustering patterns at high temperature (Fig. 3c) compared to lower temperature (Fig. 3a). As expected, aggregation occurs more slowly at lower temperature (Fig. 3d), measured by the time to aggregate to ten or fewer clusters for all runs at a given temperature. We note that the canonical scissor-twist motions of global domains within tropoelastin monomers described in earlier work [59,60] are initially present in the aggregation simulations; however, upon interaction, monomers are stabilized as the aggregation proceeds. Because cluster formation is rapid, we hypothesize that the monomeric motions contribute to self-assembly in the earliest stages of aggregation.

Coacervate nucleation occurs as monomers join together to produce growth initiation centers. Aggregation occurs from the nucleation of monomer interactions. Fig. 3e (i) shows a snapshot at the initiation of aggregation. Monomers begin to assemble via heterogeneous interactions, including head-to-tail, tail-to-tail, and lateral interactions Fig. 3e (ii-v). Nucleation events may occur as interactions between different regions of the molecule. Over time, growth of the coacervate occurs as small clusters combine into growing aggregates, forming larger coalesced structures. This behavior represents the step prior to cross-linking and polymerization in vivo. In fact, the coacervation process may serve to align tropoelastin molecules for downstream cross-linking and elastin fiber formation.

Considering the extrapolated speed-up in the CG simulations, compared to fully atomistic simulations, microsecond time scales for aggregation can be expected. It is notable that aggregation of the monomers is observed on the microsecond time scale in the CG simulations, while experimentally, coacervation is observed to occur over second time scales [61]. Through CG simulation, the dynamics of coacervation can be studied directly at the molecular scale. Coacervation is a multistep process occurring through growth of the aggregate by linear assembly of nucleation sites, as demonstrated by snapshots of aggregation (Fig. 4a–i) from initialization (Fig. 4a) to 10 μs of simulation. Heterogeneous pair formation (Fig. 3e) is followed by linear growth and cluster fusion. As the coacervate begins to grow, heterogeneous monomer pairs form through interactions of exposed hydrophobic domains. Monomer pairs form and combine with adjacent monomers or pairs to grow into small globules (Fig. 4b–e). As more monomers and pairs assemble, loose chains or fibrillar intermediates begin to form, in addition to globular structures
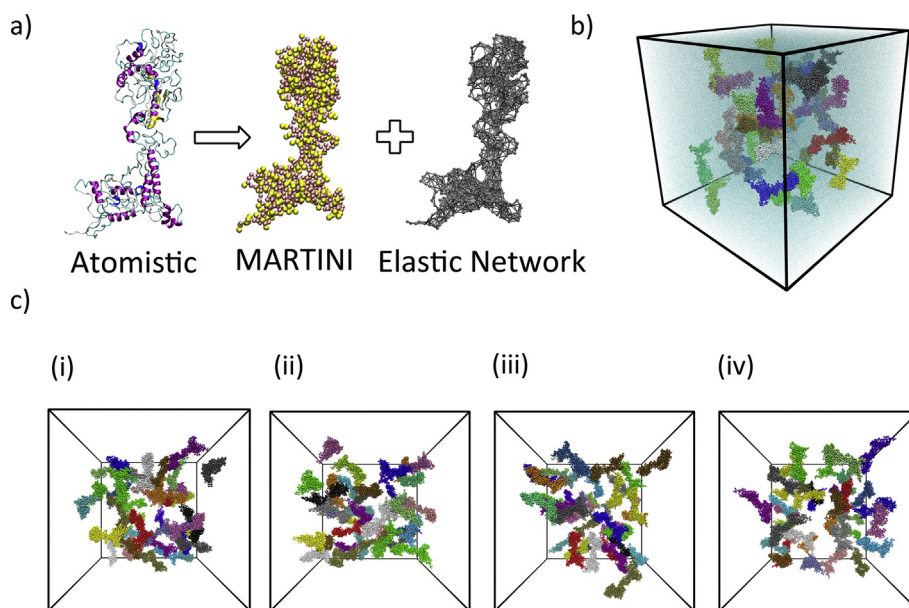
Fig. 2. (a) A coarse-grained model is constructed from the fully atomistic structure of tropoelastin from Ref. [51]. The system is coarse-grained with the MARTINI force field coupled to an elastic network model. (b) Forty tropoelastin monomers are simulated in a periodic water box. (c) Self-assembly is modeled from four distinct initial random configurations of tropoelastin monomers at each temperature.
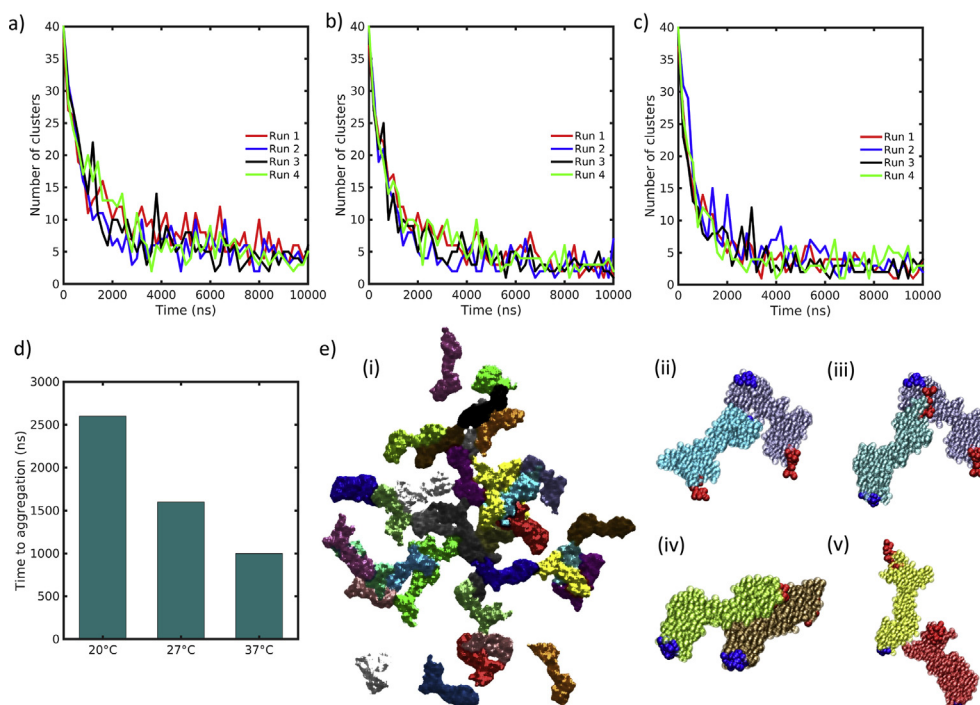
Fig. 3. Number of clusters over time in the assembly system at (a) 20 °C, (b) 27 °C, and (c) 37 °C. (d) Time to aggregation to ten or fewer clusters for all runs at 20 °C, 27 °C, and 37 °C. (e) (i) Snapshot of the tropoelastin aggregate system at 27 °C. (ii-v) Snapshots of tropoelastin monomer pairs within the aggregate from (i), with the first 20 residues highlighted in blue and last 20 residues highlighted in red. Head-to-tail, head-to-head, and lateral interactions are present in bulk clusters.

(Fig. 4f–i). The appearance of fibrillar structures at this scale suggests that elastin's filamentous structure may be reinforced in the initial stages of assembly, where cross-linking may act to stabilize the observed linear aggregates.

The nucleation and growth of tropoelastin coacervates has been characterized at micron length scales and transient submicron in vitro [2, 4,62,63]. Upon raising the temperature of tropoelastin solution to physiological temperature, coacervation begins, and the solution becomes turbid. Four distinct stages of assembly are observed: (1) formation of 70–600 nm droplets; (2) formation of 6 μm droplets; (3) fusion of droplets, and (4) a formation of a coalesced layer [37,62–65]. In simulation, cluster sizes from approximately 10 nm–70 nm in diameter are observed (Fig. 5a and b). Ten-nanometer droplets correspond to the tropoelastin monomer or dimer (Fig. 5a). As assembly proceeds, extended cluster networks up to 70 nm in diameter are observed (Fig. 5b). We expect that larger structures would be produced, given a larger simulation box; however, the present model is sufficient to capture experimentally observed aggregate sizes (Fig. 5c). In a system designed to chemically capture stabilized aggregates, tropoelastin aggregate intermediates that spanned from ~70 nm to ~600 nm were identified (Fig. 5c), confirming the presence of submicron entities during the assembly process. The nucleation and aggregation processes happen successively through coalescence, as progressively larger aggregates form through fusion of monomers or smaller clusters. The fusion process is able to proceed through the displacement of solvent molecules surrounding the monomers or aggregates. By contrast, a complementary process of Ostwald ripening [66] has also been observed under specific conditions, in particular, through the addition of sodium dodecyl sulfate to the solution of elastin-like peptides [67]. This process involves the deposition of single macromolecules onto growing aggregates through their desorption from shrinking aggregates. Interestingly, we observe that at the point of nucleation and initial growth of the aggregate from tropoelastin monomers, both fusion-based coalescence from monomers and a desorption-adsorption mechanism from smaller to intermediate nanoaggregates of the monomers are present. Accretion of tropoelastin monomers about a nucleating core is manifested dynamically through

both fusion and rearrangement of monomers and monomer clusters (Fig. 4).

Much discussion in the literature has centered around the driving forces responsible for the coacervation of tropoelastin. Hydrophobic domains within elastin have been hypothesized to drive the self-assembly process of elastin [12,21–27,30–34]. Here, the role of specific hydrophobic and hydrophilic domains within the tropoelastin monomer is analyzed. Monomers of tropoelastin in solution are driven to form clusters and aggregate into bundles through the interactions of hydrophobic domains. The role of hydrophobic domains in coacervation is demonstrated by the more pronounced reduction in the normalized solvent accessible surface area for hydrophobic domains compared to hydrophilic domains (Fig. 6a–c). The influence of hydrophobic domains on coacervation is consistent across different temperatures considered. The large central hydrophobic domains 18, 20, 24, 26, in particular, are most prominent in driving coacervation, displaying the highest solvent accessible surface area, as expected based on their sequence length compared to other domains in the monomer (Fig. 6d). When solvent accessible surface area was measured and normalized by sequence length, the larger domains did not show significant differences compared to other domains. From this, we conclude that it is the sequence length rather than the specific hydrophobic residues that is correlated to driving coacervation. The importance of domains 18 and 26 for coacervation has been demonstrated previously through characterization of mutant tropoelastin constructs [61]. The current model confirms the importance of specific domains toward self-assembly of tropoelastin.

The role of hydrophobic domains in driving self-assembly is related to the redistribution of water molecules during the assembly process. The radial distribution function of water around protein residues is shown in Fig. 6e–g for representative runs at 20, 27, and 37 °C. Over 10 μs of simulation time, the height of the sharp peaks becomes lower over time. This phenomenon is a result of the self-assembly of tropoelastin molecules, the interactions between hydrophobic domains and consequent disturbance of the water shell surrounding the protein. As tropoelastin monomers assemble, water molecules are driven away from the hydrophobic domains, becoming more disordered, represented by the drop in the radial
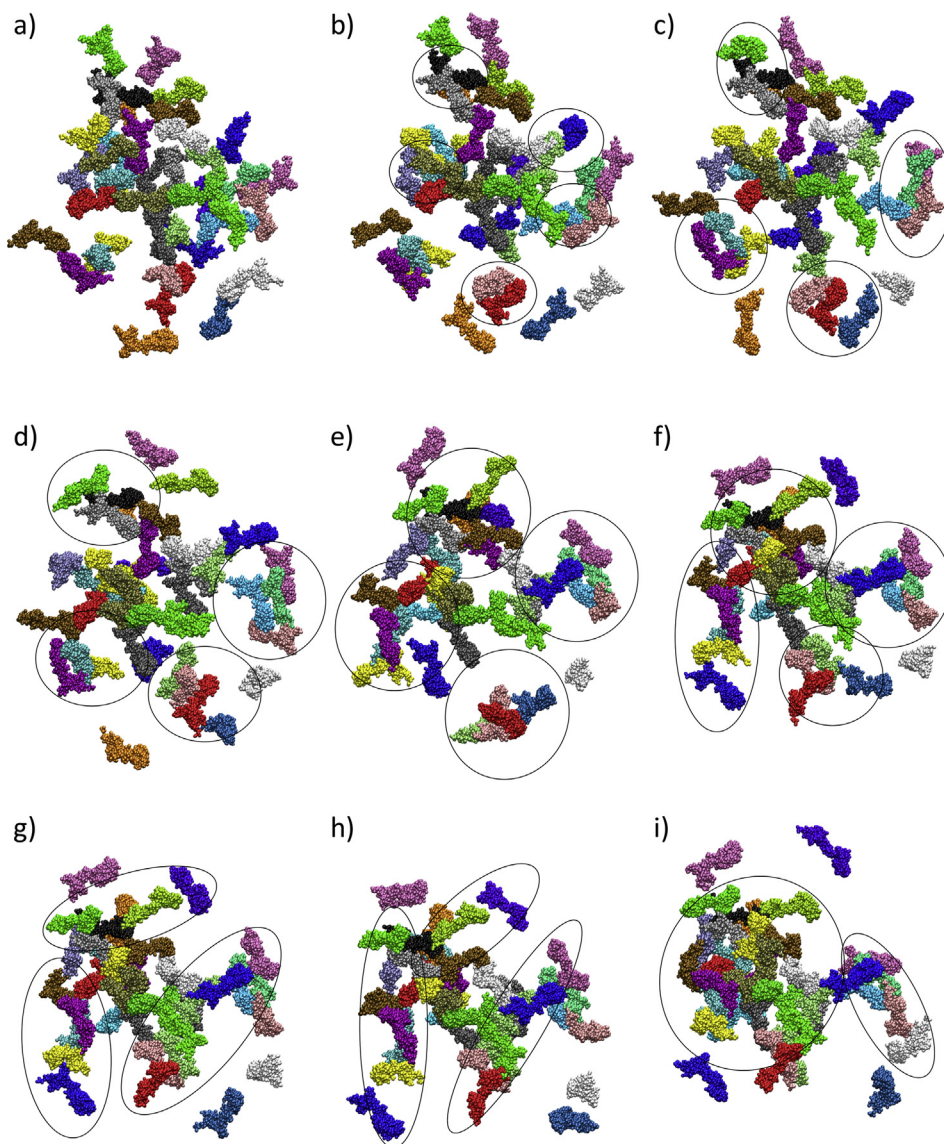
Fig. 4. Consecutive snapshots of tropoelastin assembly at 27 °C from run 2 at (a) 1 μs, (b) 2 μs, (c) 3 μs, (d) 4 μs, (e) 5 μs, (f) 6 μs, (g) 7 μs, (h) 8 μs, and (i) 9 μs. Black circles and ovals correspond to cluster initiation sites and linear cluster growth and fusion, respectively.
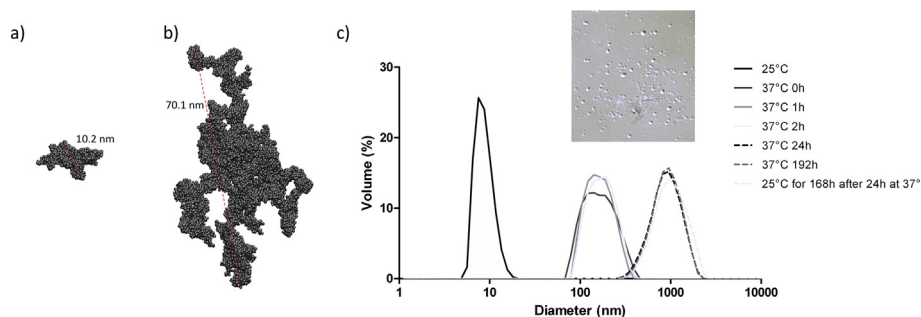
Fig. 5. Representative (a) small cluster 10.2 nm in diameter and (b) large cluster network 70.1 nm in diameter at 20 °C. (c) Particle size analysis of a 2 mg/ml tropoelastin solution at pH 10.4 over time. Inset: Stable spherical tropoelastin aggregates following a week-long incubation at 37 °C. Figure adapted with permission from Ref. [84].

distribution function peaks. This effect is reduced at higher temperature because the water shells are disturbed more easily at high temperature.

Temperature-dependent aggregation and associated phase transitions observed in this study has been well characterized for elastin and elastin-like peptides [10,11,26,68–71]. Tropoelastin and elastin-like peptides undergo reversible temperature phase transitions that are highly temperature specific as transitions occur across a narrow temperature range based on the specific sequence, molecular concentration and solvent conditions. Indeed, the models demonstrate temperature sensitivity of the system. The molecular concentration studied here is much higher in
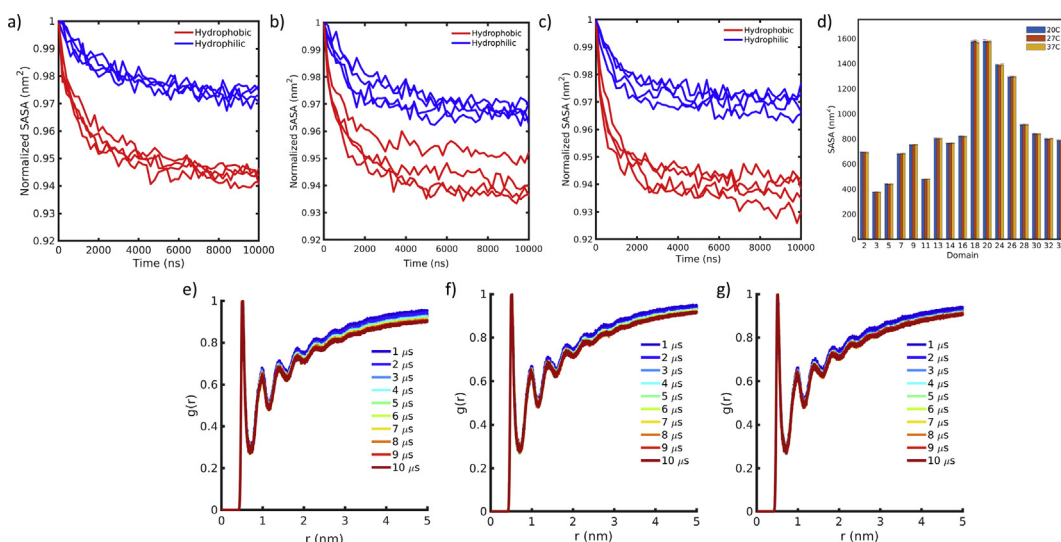
Fig. 6. | Normalized solvent accessible surface area of hydrophobic and hydrophilic domains for four runs at (a) 20 °C, (b) 27 °C, and (c) 37 °C. (d) Average solvent accessible surface area for individual hydrophobic domains at 20 °C, 27 °C, and 37 °C. Radial distribution function (RDF) (g(r)) of water beads with protein beads from 1 to 10 μs at (a) 20 °C, (b) 27 °C, and (c) 37 °C. RDF suggests that water molecules become more disordered over time.

simulation compared to experimental values, a requirement for computational expediency. So, the coacervation temperature at the experimentally observable scale can be expected to be below the temperature values studied. As would be expected, cluster formation is observed at all temperatures studied, and no significant differences in cluster size are found. Nevertheless, high temperature sensitivity is observed in the system on the microsecond scale, as demonstrated by the differences in cluster formation across different temperatures (Fig. 3a–d).

To determine the role of coacervation in orienting specific domains for downstream cross-linking, the average proximity of tropoelastin domains is calculated (Fig. 7). Snapshots at 10 μs are shown for four runs at 20 °C (Fig. 7a–d), 27 °C (Fig. 7e–h), and 37 °C (Fig. 7i–l). Proximity is

measured by the average inverse distance between domain centroids among all monomers of tropoelastin. As monomers self-assemble, a variety of interactions are observed to take place. Fig. 7 illustrates domain pair orientation states for stable clusters at the end of 10 μs of simulation, where bright yellow regions correspond to domain pairs in closest proximity. Domain pair orientations display variability in domain pair proximity. At 20 °C, proximal domain pairs for four independent runs are central hydrophobic domains and 10–19 neighboring domains (Fig. 7a); central hydrophobic domains and 19–25 neighboring domains (Fig. 7b); central hydrophobic domains, 10–19 neighboring domains and N-terminal domains (Fig. 7c); and central hydrophobic domains and 10–19 neighboring domains (Fig. 7d). At 27 °C, proximal domain pairs for four
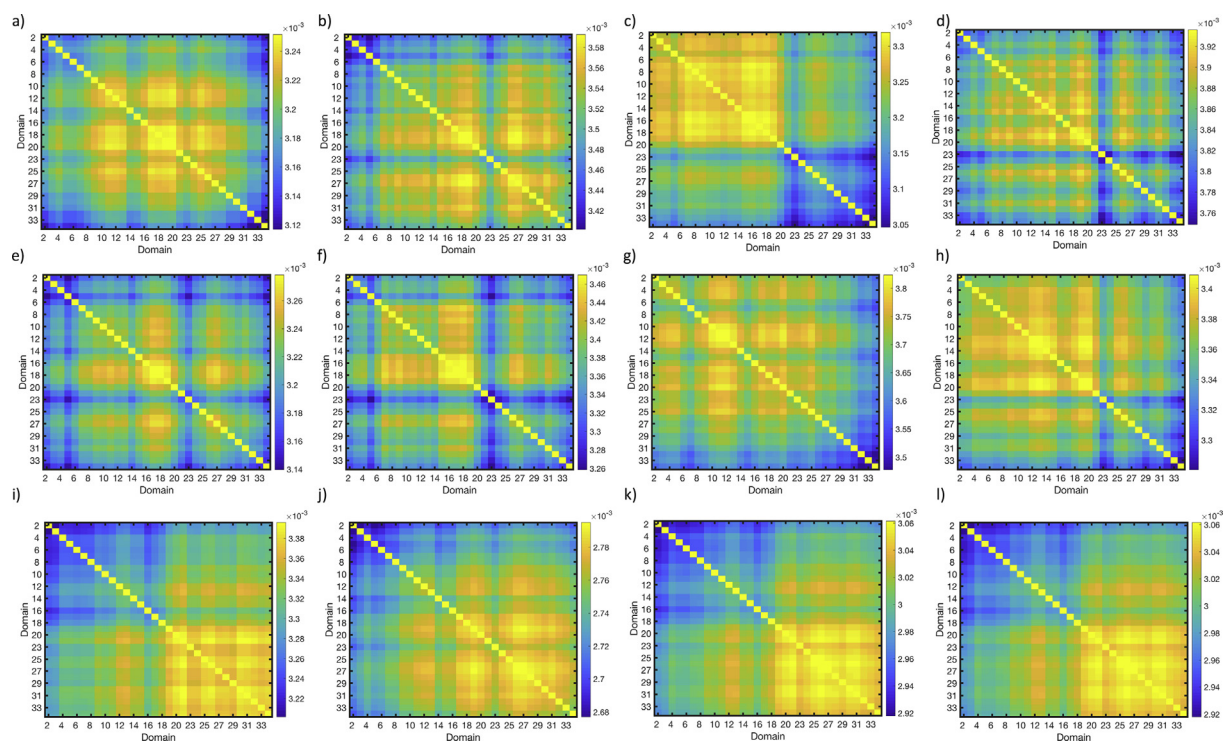
Fig. 7. Inverse distance between tropoelastin domain pair centroids at 10 μs for four independent runs, at 20 °C (a–d), 27 °C (e–h), and 37 °C (i–l). Proximity is measured by the average inverse distance between domain centroids among all monomers of tropoelastin. Yellow regions indicate most proximal domain pairs.
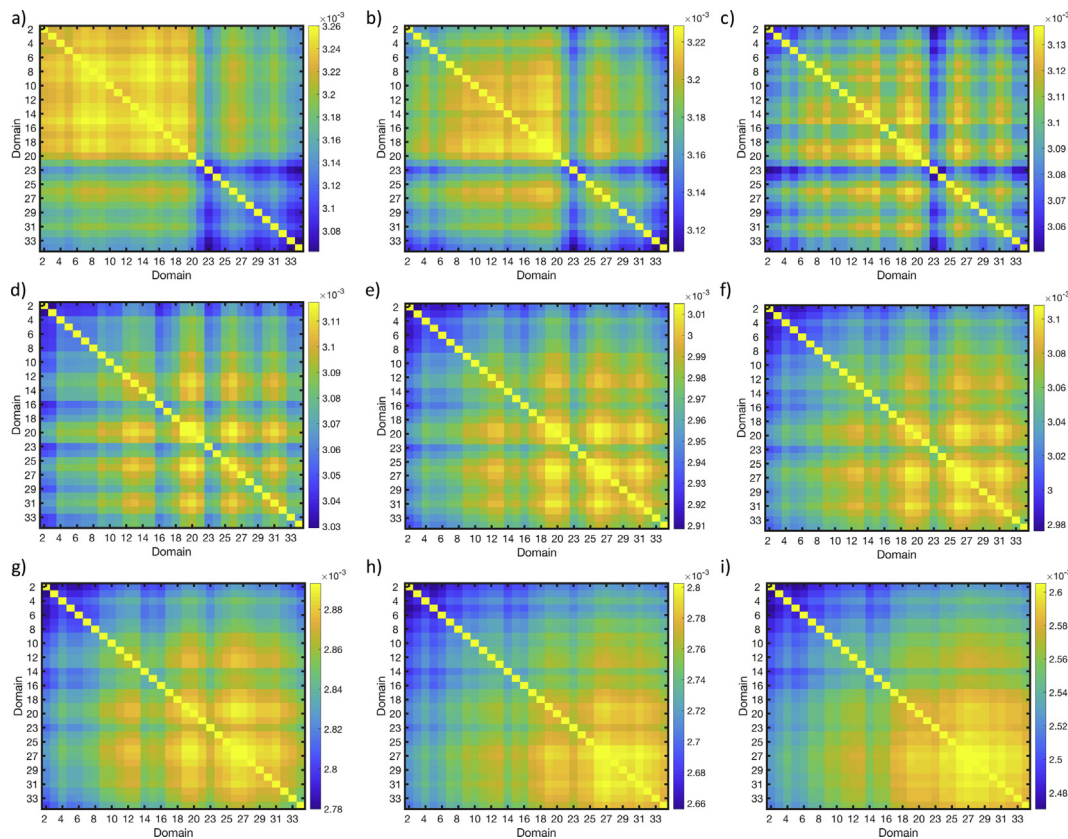
Fig. 8. Inverse distance between tropoelastin domain pair centroids at 37 °C, for run 2 at (a) 1 μs, (b) 2 μs, (c) 3 μs, (d) 4 μs, (e) 5 μs, (f) 6 μs, (g) 7 μs, (h) 8 μs, and (i) 9 μs. Proximity is measured by the average inverse distance between domain centroids among all monomers of tropoelastin. Yellow regions indicate most proximal domain pairs.

independent runs are central hydrophobic domains and 10-19-25 neighboring domains (Fig. 7e); central hydrophobic domains and 10-19-25 neighboring domains (Fig. 7f); 10–12 and 10–19 neighboring domains (Fig. 7g); and 12–14 and 10–19 neighboring domains (Fig. 7h). At 37 °C, proximal domain pairs for four independent runs are central hydrophobic domains and domain pairs in the bottom half of the molecule (Fig. 7i–l). The data at 37 °C suggest that there is a propensity for central and C-terminal domains of tropoelastin to interact upon assembly, as all four simulations are enriched in these regions (Fig. 7i–l). Considering the self-assembly pathway, domain pair proximity is independent of starting configuration and shows variability as the monomer cluster. As an example, this is clearly illustrated for sequential snapshots of domain pair distributions over the duration of one run at 27 °C (Fig. 8). Similar heterogeneity is seen for all runs and all temperatures (not shown). The high variability in domain pair proximity throughout the self-assembly process is consistent with experimental data. Mass spectrometry studies of enzymatically cleaved elastin and in vitro cross-linked recombinant human tropoelastin have proposed various regions where cross-links occur [64,72–75]. In particular, results at 37 °C support the observation that central domains may contain important sites for self-aggregation, as suggested by experimental evidence of dense cross-linking in the region 19–25 [64,75]. The most recent study mapping specific cross-linking cites suggests tropoelastin cross-linking is heterogeneous [72], a finding supported by the present model.

4. Conclusions

A model of tropoelastin self-assembly is developed through a MARTINI framework coupled with an elastic network model, from a fully atomistic structure of tropoelastin. Self-assembly of monomers is characterized at different temperatures, displaying high sensitivity. Coacervation is a stepwise process where self-assembled structures display both fibrillar and globular substructures within the bulk. It is hypothesized that linear formations during aggregation may act to strengthen elastin fibers upon higher level assembly. The model captures temperature specificity of the assembly process and reinforces the role of specific hydrophobic domains as assembly drivers. Coacervation proceeds through the interaction of hydrophobic domains and the reordering of water molecules around aggregates. The model predicts heterogeneous domain pair orientations during the self-assembly process, consistent with the heterogeneous cross-linking identified within elastin.

The present model is most faithful to a representation of in vitro tropoelastin coacervation, as several features of in vivo coacervation are not accounted for. However, it would be important to implement those in future work. In particular, tropoelastin coacervation is observed to take place on the cell surface in the extracellular space with tropoelastin coacervates attached to the cell surface integrins and glycosaminoglycans, which may facilitate the coacervation process [62,76]. Aggregation facilitated by integrins, glycosaminoglycans, microfibrillar and other proteins may be incorporated into future models. We note also that the model does not explicitly capture changes in secondary structure upon aggregation. Further, although the elastic network contributes to stabilizing the tropoelastin molecule, we acknowledge that the effect of the network may limit the flexibility of the molecule. Still, the present model relies on the overall shape of the tropoelastin molecule and the primary sequence, simulating accurately previous experimental results. As tropoelastin is deposited on the microfibrillar scaffold, interactions with microfibrillar proteins are likely to further promote coacervation and direct coacervate alignment and fiber orientation [77–82].

Declaration of interests

The authors declare that they have no known competing financial interests or personal relationships that could have appeared to influence the work reported in this paper.

Acknowledgments

Appendix A. Supplementary data

Supplementary data to this article can be found online at https://doi.org/10.1016/j.mtbio.2019.100016.

References

[1] S.G. Wise, A.S. Weiss, Tropoelastin, Int. J. Biochem. Cell Biol. 41 (3) (2009) 494–497.

[2] J.E. Wagenseil, R.P. Mecham, New insights into elastic fiber assembly, Birth Defects Res. C Embryo Today 81 (4) (2007) 229–240.

[3] B. Vrhovski, A.S. Weiss, Biochemistry of tropoelastin, Eur. J. Biochem. 258 (1) (1998) 1–18.

[4] G.C. Yeo, F.W. Keeley, A.S. Weiss, Coacervation of tropoelastin, Adv. Colloid Interface Sci. 167 (2011) 94–103.

[5] A.K. Baldwin, A. Simpson, R. Steer, S.A. Cain, C.M. Kielty, Elastic fibres in health and disease, Expert Rev. Mol. Med. 15 (2013).

[6] A.S. Narayanan, R.C. Page, F. Kuzan, C.G. Cooper, Elastin cross-linking in vitro. Studies on factors influencing the formation of desmosines by lysyl oxidase action on tropoelastin, Biochem. J. 173 (3) (1978) 857–862.

[7] A.W. Clarke, et al., Tropoelastin massively associates during coacervation to form quantized protein spheres, Biochemistry 45 (33) (2006) 9989–9996.

[8] B.A. Kozel, et al., Elastic fiber formation: a dynamic view of extracellular matrix assembly using timer reporters, J. Cell. Physiol. 207 (1) (2006) 87–96.

[9] L. Debelle, A.M. Tamburro, Elastin: molecular description and function, Int. J. Biochem. Cell Biol. 31 (2) (1999) 261–272.

[10] C.L. DW Urry, T.M. Parker, D.C. Gowda, K.U. Prasad, M.C. Reid, A. Safavy, Temperature of polypeptide inverse temperature transition depends on mean residue hydrophobicity, J. Am. Chem. Soc. 113 (1991) 4346–4348.

[11] D.W. Urry, et al., Hydrophobicity scale for proteins based on inverse temperature transitions, Biopolymers 32 (9) (1992) 1243–1250.

[12] B.A. Cox, B.C. Starcher, D.W. Urry, Communication: coacervation of tropoelastin results in fiber formation, J. Biol. Chem. 249 (3) (1974) 997–998.

[13] D.W. Urry, B. Starcher, S.M. Partridge, Coacervation of solubilized elastin effects a notable conformational change, Nature 222 (5195) (1969) 795–796.

[14] K. Kaibara, T. Watanabe, K. Miyakawa, Characterizations of critical processes in liquid-liquid phase separation of the elastomeric protein-water system: microscopic observations and light scattering measurements, Biopolymers 53 (5) (2000) 369–379.

[15] G.M. Bressan, et al., Banded fibers in tropoelastin coacervates at physiological temperatures, J. Ultrastruct. Res. 82 (3) (1983) 335–340.

[16] G.M. Bressan, et al., Relevance of aggregation properties of tropoelastin to the assembly and structure of elastic fibers, J. Ultrastruct. Mol. Struct. Res. 94 (3) (1986) 209–216.

[17] J.T. Cirulis, et al., Fibrillins, fibulins, and matrix-associated glycoprotein modulate the kinetics and morphology of in vitro self-assembly of a recombinant elastin-like polypeptide, Biochemistry 47 (47) (2008) 12601–12613.

[18] S.M. Partridge, H.F. Davis, G.S. Adair, The chemistry of connective tissues. 2. Soluble proteins derived from partial hydrolysis of elastin, Biochem. J. 61 (1) (1955) 11–21.

[19] A.M. Jamieson, C.E. Downs, A.G. Walton, Studies of elastin coacervation by quasielastic light scattering, Biochim. Biophys. Acta 271 (1) (1972) 34–47.

[20] A.M. Jamieson, B. Simic-Glavaski, K. Tansey, A.G. Walton, Studies of elastin coacervation by quasielastic light scattering, Faraday Discuss. Chem. Soc. 61 (1976) 194–204.

[21] M.A. Morelli, M. DeBiasi, A. DeStradis, A.M. Tamburro, An aggregating elastin-like pentapeptide, J. Biomol. Struct. Dyn. 11 (1) (1993) 181–190.

[22] H. Reiersen, A.R. Clarke, A.R. Rees, Short elastin-like peptides exhibit the same temperature-induced structural transitions as elastin polymers: implications for protein engineering, J. Mol. Biol. 283 (1) (1998) 255–264.

[23] A.M. Tamburro, V. Guantieri, D.D. Gordini, Synthesis and structural studies of a pentapeptide sequence of elastin. Poly (Val-Gly-Gly-Leu-Gly), J. Biomol. Struct. Dyn. 10 (3) (1992) 441–454.

[24] M.M. Long, R.S. Rapaka, D. Volpin, I. Pasquali-Ronchetti, D.W. Urry, Spectroscopic and electron micrographic studies on the repeat tetrapeptide of tropoelastin: (Val-Pro-Gly-Gly)n, Arch. Biochem. Biophys. 201 (2) (1980) 445–452.

[25] C.H. Luan, R.D. Harris, K.U. Prasad, D.W. Urry, Differential scanning calorimetry studies of the inverse temperature transition of the polypentapeptide of elastin and its analogues, Biopolymers 29 (14) (1990) 1699–1706.

[26] D.W. Urry, Entropic elastic processes in protein mechanisms. I. Elastic structure due to an inverse temperature transition and elasticity due to internal chain dynamics, J. Protein Chem. 7 (1) (1988) 1–34.

[27] D.W. Urry, T.L. Trapane, K.U. Prasad, Phase-structure transitions of the elastin polypentapeptide-water system within the framework of composition-temperature studies, Biopolymers 24 (12) (1985) 2345.

[28] S. Singh, et al., Coacervation of elastin-like recombinamer microgels, Macromol. Rapid Commun. 37 (2) (2016) 181–186.

[29] I. Gonzalez de Torre, L. Quintanilla, G. Pinedo-Martin, M. Alonso, J.C. Rodriguez-Cabello, Nanogel formation from dilute solutions of clickable elastin-like recombinamers and its dependence on temperature: two fractal gelation modes, ACS Appl. Mater. Interfaces 6 (16) (2014) 14509–14515.

[30] A. Pepe, et al., Dissection of human tropoelastin: supramolecular organization of polypeptide sequences coded by particular exons, Matrix Biol. 24 (2) (2005) 96–109.

[31] D.C. Gowda, et al., Synthesis and characterization of the human elastin W4 sequence, Int. J. Pept. Protein Res. 46 (6) (1995) 453–463.

[32] C.M. Bellingham, K.A. Woodhouse, P. Robson, S.J. Rothstein, F.W. Keeley, Self-aggregation characteristics of recombinantly expressed human elastin polypeptides, Biochim. Biophys. Acta 1550 (1) (2001) 6–19.

[33] M. Miao, et al., Sequence and structure determinants for the self-aggregation of recombinant polypeptides modeled after human elastin, J. Biol. Chem. 278 (49) (2003) 48553–48562.

[34] A. Pepe, et al., Exon 26-coded polypeptide: an isolated hydrophobic domain of human tropoelastin able to self-assemble in vitro, Matrix Biol. 27 (5) (2008) 441–450.

[35] F.W. Keeley, C.M. Bellingham, K.A. Woodhouse, Elastin as a self-organizing biomaterial: use of recombinantly expressed human elastin polypeptides as a model for investigations of structure and self-assembly of elastin, Philos T R Soc B 357 (1418) (2002) 185–189.

[36] M. Miao, J.T. Cirulis, S. Lee, F.W. Keeley, Structural determinants of cross-linking and hydrophobic domains for self-assembly of elastin-like polypeptides, Biochemistry 44 (43) (2005) 14367–14375.

[37] B. Vrhovski, S. Jensen, A.S. Weiss, Coacervation characteristics of recombinant human tropoelastin, Eur. J. Biochem. 250 (1) (1997) 92–98.

[38] W.J. Wu, B. Vrhovski, A.S. Weiss, Glycosaminoglycans mediate the coacervation of human tropoelastin through dominant charge interactions involving lysine side chains, J. Biol. Chem. 274 (31) (1999) 21719–21724.

[39] C.M. Bellingham, et al., Recombinant human elastin polypeptides self-assemble into biomaterials with elastin-like properties, Biopolymers 70 (4) (2003) 445–455.

[40] B. Li, D.O.V. Alonso, B.J. Bennion, V. Daggett, Hydrophobic hydration is an important source of elasticity in elastin-based biopolymers, J. Am. Chem. Soc. 123 (48) (2001) 11991–11998.

[41] B. Li, D.O.V. Alonso, V. Daggett, The molecular basis for the inverse temperature transition of elastin, J. Mol. Biol. 305 (3) (2001) 581–592.

[42] R. Rousseau, E. Schreiner, A. Kohlmeyer, D. Marx, Temperature-dependent conformational transitions and hydrogen-bond dynamics of the elastin-like octapeptide GVG(VPGVG): a molecular-dynamics study, Biophys. J. 86 (3) (2004) 1393–1407.

[43] A. Tarakanova, M.J. Buehler, Molecular modeling of protein materials: case study of elastin, Model. Simul .Mater. Sc. 21 (6) (2013).

[44] A. Tarakanova, W. Huang, A.S. Weiss, D.L. Kaplan, M.J. Buehler, Computational smart polymer design based on elastin protein mutability, Biomaterials 127 (2017) 49–60.

[45] D.K. Chang, D.W. Urry, Molecular dynamics calculations on relaxed and extended states of the polypentapeptide of elastin, Chem. Phys. Lett. 147 (4) (1988) 395–400.

[46] F. Lelj, A.M. Tamburro, V. Villani, P. Grimaldi, V. Guantieri, Molecular dynamics study of the conformational behavior of a representative elastin building block: boc-Gly-Val-Gly-Gly-Leu-OMe, Biopolymers 32 (2) (1992) 161–172.

[47] S. Rauscher, S. Baud, M. Miao, F.W. Keeley, R. Pomes, Proline and glycine control protein self-organization into elastomeric or amyloid fibrils, Structure 14 (11) (2006) 1667–1676.

[48] J.E. Condon, T.B. Martin, A. Jayaraman, Effect of conjugation on phase transitions in thermoresponsive polymers: an atomistic and coarse-grained simulation study, Soft Matter 13 (16) (2017) 2907–2918.

[49] N.K. Li, F. García Quiroz, C.K. Hall, A. Chilkoti, Y.G. Yingling, Molecular description of the LCST behavior of an elastin-like polypeptide, Biomacromolecules 15 (10) (2014) 3522–3530.

[50] S. Rauscher, R. Pomes, The liquid structure of elastin, Elife 6 (2017).

[51] A. Tarakanova, G.C. Yeo, C. Baldock, A.S. Weiss, M.J. Buehler, Molecular model of human tropoelastin and implications of associated mutations, Proc. Natl. Acad. Sci. Unit. States Am. 115 (28) (2018) 7338–7343.

[52] D.H. de Jong, et al., Improved parameters for the martini coarse-grained protein force field, J. Chem. Theory Comput. 9 (1) (2013) 687–697.

[53] S.J. Marrink, H.J. Risselada, S. Yefimov, D.P. Tieleman, A.H. de Vries, The MARTINI force field: coarse grained model for biomolecular simulations, J. Phys. Chem. B 111 (27) (2007) 7812–7824.

[54] X. Periole, M. Cavalli, S.J. Marrink, M.A. Ceruso, Combining an elastic network with a coarse-grained molecular force field: structure, dynamics, and intermolecular recognition, J. Chem. Theory Comput. 5 (9) (2009) 2531–2543.

[55] L. Monticelli, et al., The MARTINI coarse-grained force field: extension to proteins, J. Chem. Theory Comput. 4 (5) (2008) 819–834.

[56] B. Hess, C. Kutzner, D. van der Spoel, E. Lindahl, GROMACS 4: algorithms for highly efficient, load-balanced, and scalable molecular simulation, J. Chem. Theory Comput. 4 (3) (2008) 435–447.

[57] D. Van Der Spoel, et al., GROMACS: fast, flexible, and free, J. Comput. Chem. 26 (16) (2005) 1701–1718.

[58] W. Humphrey, A. Dalke, K. Schulten, VMD: Visual molecular dynamics, J. Mol. Graph. 14 (33) (1996).

[59] G.C. Yeo, et al., Subtle balance of tropoelastin molecular shape and flexibility regulates dynamics and hierarchical assembly, Sci Adv 2 (2) (2016) e1501145.

[60] A. Tarakanova, G.C. Yeo, C. Baldock, A.S. Weiss, M.J. Buehler, Tropoelastin is a flexible molecule that retains its canonical shape, Macromol. Biosci. 19 (3) (2019) e1800250.

[61] P. Toonkool, S.A. Jensen, A.L. Maxwell, A.S. Weiss, Hydrophobic domains of human tropoelastin interact in a context-dependent manner, J. Biol. Chem. 276 (48) (2001) 44575–44580.

[62] Y. Tu, A.S. Weiss, Glycosaminoglycan-mediated coacervation of tropoelastin abolishes the critical concentration, accelerates coacervate formation, and facilitates spherule fusion: implications for tropoelastin microassembly, Biomacromolecules 9 (7) (2008) 1739–1744.

[63] Y. Tu, A.S. Weiss, Transient tropoelastin nanoparticles are early-stage intermediates in the coacervation of human tropoelastin whose aggregation is facilitated by heparan sulfate and heparin decasaccharides, Matrix Biol. 29 (2) (2010) 152–159.

[64] S.M. Mithieux, S.G. Wise, M.J. Raftery, B. Starcher, A.S. Weiss, A model two-component system for studying the architecture of elastin assembly in vitro, J. Struct. Biol. 149 (3) (2005) 282–289.

[65] Y. Tu, S.G. Wise, A.S. Weiss, Stages in tropoelastin coalescence during synthetic elastin hydrogel formation, Micron 41 (3) (2010) 268–272.

[66] P. Taylor, Ostwald ripening in emulsions, Adv. Colloid Interface Sci. 75 (1998) 107–163.

[67] Y. Zhang, K. Trabbic-Carlson, F. Albertorio, A. Chilkoti, P.S. Cremer, Aqueous two-phase system formation kinetics for elastin-like polypeptides of varying chain length, Biomacromolecules 7 (7) (2006) 2192–2199.

[68] L. Martin, E. Castro, A. Ribeiro, M. Alonso, J.C. Rodriguez-Cabello, Temperature-triggered self-assembly of elastin-like block co-recombinamers:the controlled formation of micelles and vesicles in an aqueous medium, Biomacromolecules 13 (2) (2012) 293–298.

[69] A. Chilkoti, M.R. Dreher, D.E. Meyer, Design of thermally responsive, recombinant polypeptide carriers for targeted drug delivery, Adv. Drug Deliv. Rev. 54 (8) (2002) 1093–1111.

[70] T. Christensen, W. Hassouneh, K. Trabbic-Carlson, A. Chilkoti, Predicting transition temperatures of elastin-like polypeptide fusion proteins, Biomacromolecules 14 (5) (2013) 1514–1519.

[71] J.R. McDaniel, D.C. Radford, A. Chilkoti, A unified model for de novo design of elastin-like polypeptides with tunable inverse transition temperatures, Biomacromolecules 14 (8) (2013) 2866–2872.

[72] C.U. Schrader, et al., Elastin is heterogeneously cross-linked, J. Biol. Chem. 293 (39) (2018) 15107–15119.

[73] P. Brown-Augsburger, C. Tisdale, T. Broekelmann, C. Sloan, R.P. Mecham, Identification of an elastin cross-linking domain that joins three peptide chains. Possible role in nucleated assembly, J. Biol. Chem. 270 (30) (1995) 17778–17783.

[74] A. Heinz, et al., Molecular-level characterization of elastin-like constructs and human aortic elastin, Matrix Biol. : J. Int. Soc. Matrix Biol. 38 (2014) 12–21.

[75] S.G. Wise, S.M. Mithieux, M.J. Raftery, A.S. Weiss, Specificity in the coacervation of tropoelastin: solvent exposed lysines, J. Struct. Biol. 149 (3) (2005) 273–281.

[76] T.J. Broekelmann, et al., Tropoelastin interacts with cell-surface glycosaminoglycans via its COOH-terminal domain, J. Biol. Chem. 280 (49) (2005) 40939–40947.

[77] R.P. Mecham, Elastin synthesis and fiber assembly, Ann. N. Y. Acad. Sci. 624 (1991) 137–146.

[78] M. Hirai, et al., Fibulin-5/DANCE has an elastogenic organizer activity that is abrogated by proteolytic cleavage in vivo, J. Cell Biol. 176 (7) (2007) 1061–1071.

[79] T. Nakamura, et al., Fibulin-5/DANCE is essential for elastogenesis in vivo, Nature 415 (6868) (2002) 171–175.

[80] R. Nonaka, et al., DANCE/fibulin-5 promotes elastic fiber formation in a tropoelastin isoform-dependent manner, Clin. Biochem. 42 (7–8) (2009) 713–721.

[81] M.J. Rock, et al., Molecular basis of elastic fiber formation. Critical interactions and a tropoelastin-fibrillin-1 cross-link, J. Biol. Chem. 279 (22) (2004) 23748–23758.

[82] A.W. Clarke, S.G. Wise, S.A. Cain, C.M. Kielty, A.S. Weiss, Coacervation is promoted by molecular interactions between the PF2 segment of fibrillin-1 and the domain 4 region of tropoelastin, Biochemistry 44 (30) (2005) 10271–10281.

[83] J. Towns, et al., XSEDE: accelerating scientific Discovery, Comput. Sci. Eng. 16 (5) (2014) 62–74.

[84] S.M. Mithieux, Y. Tu, E. Korkmaz, F. Braet, A.S. Weiss, In situ polymerization of tropoelastin in the absence of chemical cross-linking, Biomaterials 30 (4) (2009) 431–435.